Making conjugated connections to porphyrins: a comparison of alkyne, alkene, imine and azo links

Thomas E. O. Screen,[a] Iain M. Blake,[a] Leigh H. Rees,[b] William Clegg,[c] Simon J. Borwick[b] and Harry L. Anderson*[a]

[a] *Department of Chemistry, University of Oxford, Dyson Perrins Laboratory, South Parks Road, Oxford, UK OX1 3QY. E-mail: harry.anderson@chem.ox.ac.uk*
[b] *Department of Chemistry, University of Oxford, Chemical Crystallography Laboratory, 9 Parks Road, Oxford, UK OX1 3PD*
[c] *Department of Chemistry, University of Newcastle, Newcastle upon Tyne, UK NE1 7RU*

Received (in Cambridge, UK) 30th October 2001, Accepted 12th December 2001
First published as an Advance Article on the web 10th January 2002

A series of porphyrins **5**–**9** has been prepared, in which an aryl substituent is linked to the porphyrin *via* azo, imine, alkene and alkyne bridges. The strength of aryl–porphyrin electronic coupling in these systems was evaluated from the red shift and intensification of the Q band absorption and emission spectra, and from the incremental red shift on changing from the phenyl to a 4-nitrophenyl substituent. The azo link provides the strongest electronic communication between the porphyrin and the benzene ring. The crystal structures of azo compounds **5a** and **5c** show that the porphyrin and benzene rings are almost coplanar, whereas imine **7a** and alkene **8a** are significantly twisted in the solid state. Imine and alkyne linked porphyrin dimers **18** and **23** were also synthesized; the alkyne-linked dimer is much more conjugated than its imine-linked analogue.

Introduction

Porphyrin-based electronic materials continue to attract attention because of their unusual electro-optical and nonlinear optical (NLO) behaviour.[1] Work by several research teams has led to the conclusion that acetylenic *meso*-substituents provide the most efficient way of making conjugated connections to porphyrin π-systems. For example, Therien and coworkers have shown that donor–acceptor aryl-ethynyl porphyrins such as **1** have much higher second order NLO coefficients than analogous *meso*-aryl porphyrins,[2,3] while we have shown that the strong inter-porphyrin conjugation in butadiyne-linked porphyrin oligomers results in exceptional third order NLO behaviour.[4,5] *meso*-Tetraalkynylporphyrins are also remarkable for their sharp red-shifted absorption spectra[6–9] and strong optical limiting in the visible region.[10]

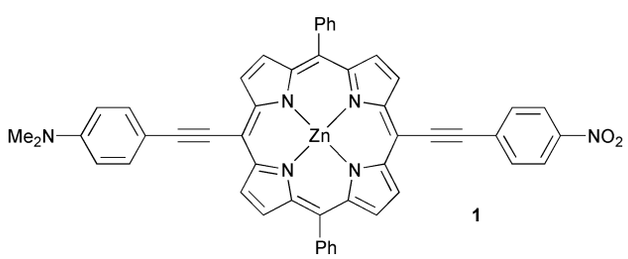

1

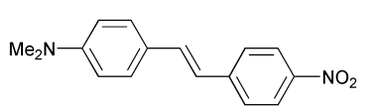

2

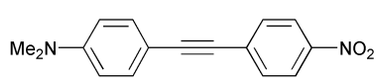

3

The pre-eminence of alkyne links in this area contrasts with the emerging design principles in the wider field of conjugated organic materials, where alkene links generally provide stronger electronic communication than alkynes.[11–13] For example stilbene **2** exhibits more red-shifted absorption maxima and larger 2nd and 3rd order NLO coefficients than its tolan (diphenylacetylene) analogue **3**.[14] This is attributed to poor sp^1–sp^2 π-overlap, due to the energy mismatch between the *p*-orbitals on sp^1 and sp^2 carbon atoms.[15] Alkyne-links achieve higher conjugation in porphyrin-based materials because they allow planar π-overlap whereas aryl or alkene-links twist out of conjugation, due to steric interactions with the *β*-pyrrole substituents. Changing the atom attached at the porphyrin *meso* position to nitrogen should also remove this steric clash. An azo substituent is iso-electronic with an alkene, and almost as slim as an alkyne, which suggests that it may be interesting to explore the chemistry of *meso* azo-linked porphyrins. Azo-linked porphyrins such as **4** have also been predicted to have strong NLO behaviour,[16] but the synthesis of compounds of this type has not been reported.

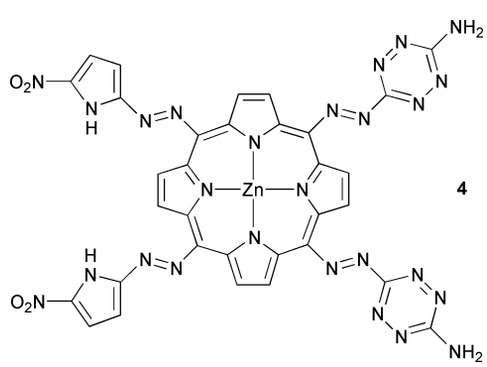

4

Imines are generally easier to prepare than azo compounds, and an imine link might be expected to have properties intermediate between an azo and an alkene. However it has long been known that whereas *E*-stilbenes and *E*-azobenzenes are roughly planar, *E*-benzalanilines (Ar–N=CH–Ph) are twisted. The *N*-aryl ring is at an angle of about 50° to the plane of the N=CH–Ph group, as revealed in the solid state by X-ray crystallography,[17] in the gas phase by electron diffraction[18] and in

 DOI: 10.1039/b109915a

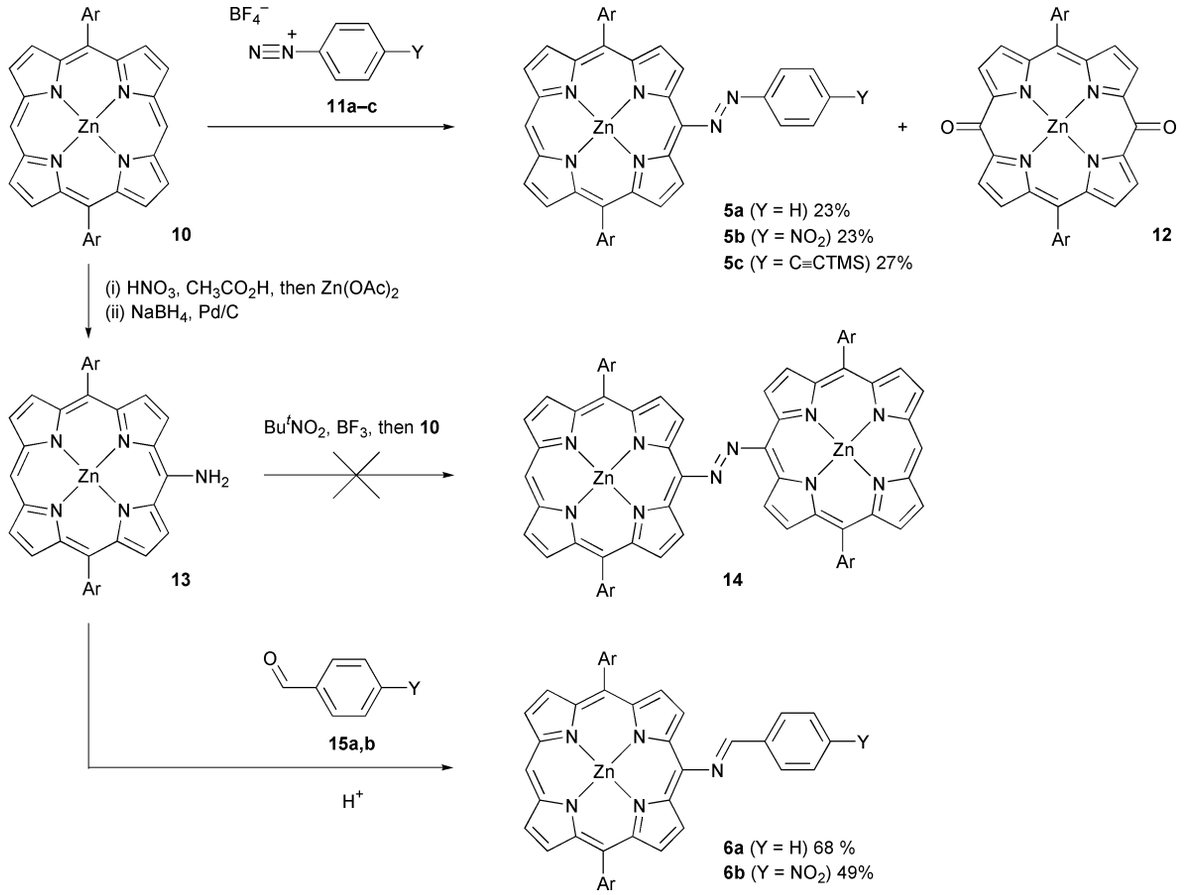

Scheme 1 Ar = 3,5-Bu$^t_2$C$_6$H$_3$; **a**: Y = H; **b**: Y = NO$_2$; **c**: Y = C≡CSiMe$_3$.

solution by CNDO/S CI (complete neglect of differential overlap configuration interaction) simulation of UV spectra.[19] This nonplanarity results in weaker conjugation in imine-linked systems.[20] We set out to explore this effect in *meso* imine-linked porphyrins.

Here we present a survey of *meso*-substituted porphyrins with alkyne, alkene, imine and azo links. To the best of our knowledge, this is the first synthesis of *meso*-azo-arylporphyrins such as **5a**–**c**. There is only one previous report[21] of *meso*-imine-arylporphyrins such as **6a**,**b** and **7a**,**b**, and these previous imines had *β*-pyrrolic alkyl substituents, making them much less conjugated. We have also prepared *meso*-ethene-arylporphyrins **8a**,**b** and *meso*-ethynyl-arylporphyrins **9a**,**b** for comparison. Here we also compare the properties of imine-linked and acetylene-linked porphyrin dimers.

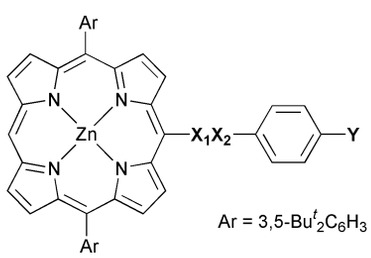

5a (X_1X_2 = N=N; Y = H)
5b (X_1X_2 = N=N; Y = NO$_2$)
5c (X_1X_2 = N=N; Y = C$_2$TMS)
6a (X_1X_2 = N=CH; Y = H)
6b (X_1X_2 = N=CH; Y = NO$_2$)
7a (X_1X_2 = CH=N; Y = H)
7b (X_1X_2 = CH=N; Y = NO$_2$)
8a (X_1X_2 = CH=CH; Y = H)
8b (X_1X_2 = CH=CH; Y = NO$_2$)
9a (X_1X_2 = C≡C; Y = H)
9b (X_1X_2 = C≡C; Y = NO$_2$)

The strength of porphyrin–aryl conjugation was assessed by comparing the absorption and emission spectra of these compounds, and by crystallographic and computational analysis of their geometries.

Results and discussion

Synthesis

Porphyrin azo dyes **5a**–**c** were prepared by treating zinc porphyrin **10** with aryldiazonium tetrafluoroborates **11a**–**c**[22] in THF at room temperature (Scheme 1). The reaction is fastest with the most electrophilic 4-nitrophenyl diazonium salt **11b**. The dioxo-porphyrin **12** was also isolated as a by-product from all three reactions, while the desired product was isolated in 23–27% yield. No disubstituted products were formed, even when using a large excess of the diazonium salt, due to the strongly electron-withdrawing effect of the azo substituent.

Many types of aromatic electrophilic substitution have been reported with porphyrins,[23] but as far as we are aware there have been no previous reports of azo coupling. An alternative route to porphyrin azo dyes would be to react a porphyrin diazonium salt with an electron-rich aromatic unit. There is only one previous report of the synthesis of a porphyrin *meso*-diazonium salt, and this was used for Sandmeyer halogenation rather than azo-coupling.[24] We prepared a *meso*-aminoporphyrin **13** *via* nitration of **10** (Scheme 1) but all attempts at making the diazonium salt from this, and its subsequent reaction with porphyrin **10** to give dimer **14**, were unsuccessful.

Imine linked porphyrin-aryl compounds **6a** and **6b** were prepared in 68% and 49% yields by condensing aminoporphyrin **13** with benzaldehydes **15a** and **15b** (Scheme 1). Compound **13** was refluxed over 4 Å molecular sieves in the presence of an excess of benzaldehyde and Amberlyst 15 macroreticular ion-exchange resin as catalyst. With **6b**, difficult removal of excess unreacted 4-nitrobenzaldehyde reduced the yield. For the isomeric imines **7a** and **7b**, formylporphyrin **16** was prepared *via* Vilsmeier formylation of **10**, then reaction with anilines **17a** and **17b** to give **7a** and **7b** in 78% and 85% yields (Scheme 2). Imine linked porphyrin dimer **18** was prepared under analogous conditions from formylporphyrin **16** and aminoporphyrin **13**.

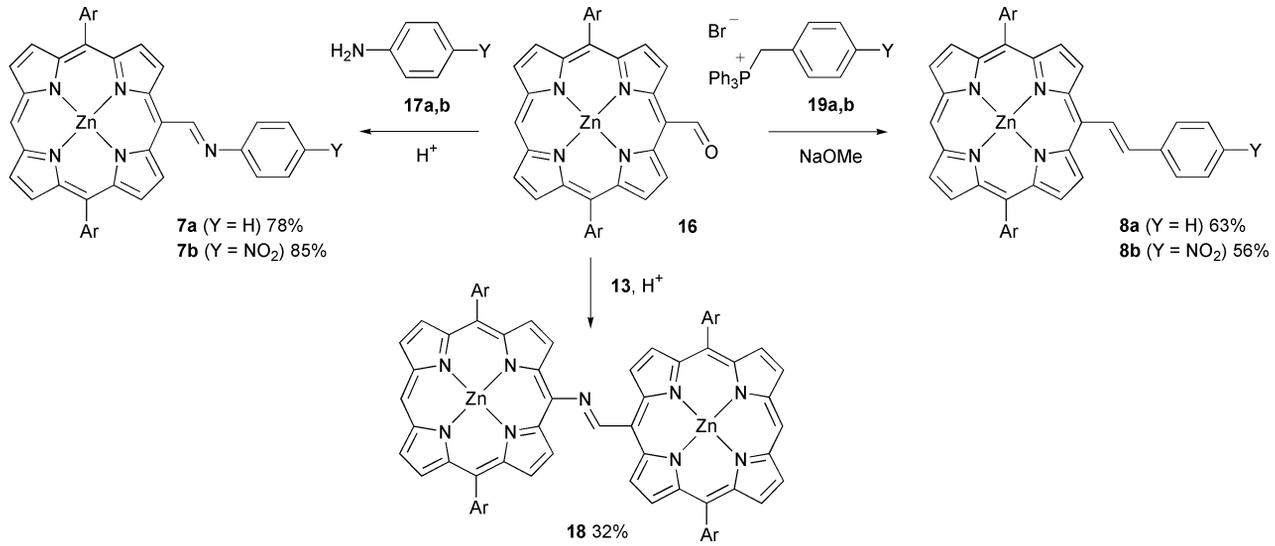

Scheme 2 Ar = 3,5-Bu$^t_2$C$_6$H$_3$; **a**: Y = H; **b**: Y = NO$_2$.

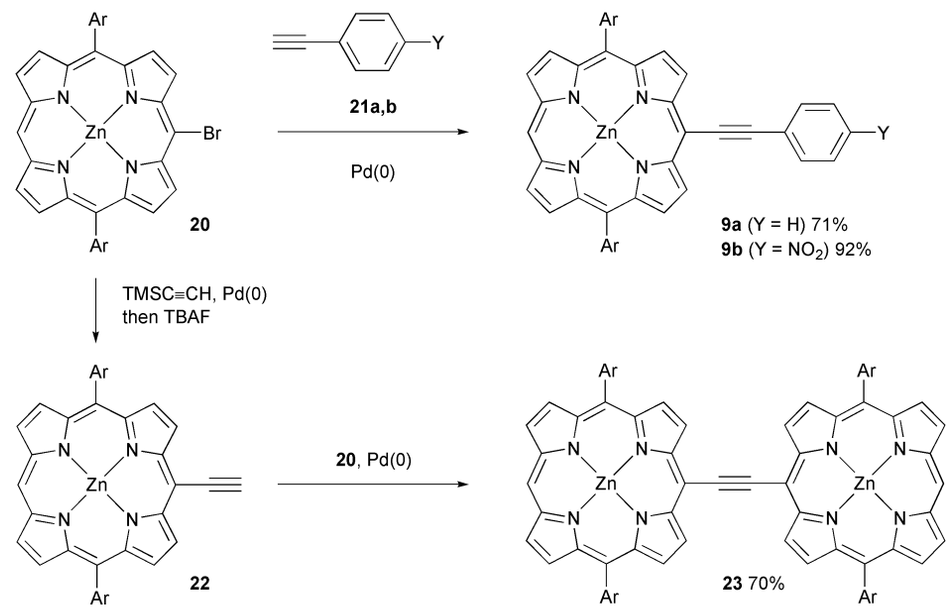

Scheme 3 Ar = 3,5-Bu$^t_2$C$_6$H$_3$; **a**: Y = H; **b**: Y = NO$_2$.

This gave **18** in 32% yield. The disappointing yield of dimer may be due to degradation of the aminoporphyrin during the long reaction time.

The ethene linked *meso*-arylporphyrins **8a** and **8b** were formed by Wittig reaction between **16** and phosphonium salts **19a** and **19b** (Scheme 2). *meso* CH=CH–Ar porphyrins have previously been prepared as intermediates to ethane linked photosynthetic models by Nishitani *et al.*,[25] and in low yield from pyrrole and cinnamaldehyde by Czuchajowski *et al.*,[26] but neither investigation addressed the extent of conjugation across the ethene link. *meso*-Ethynylporphyrins **9a** and **9b** were prepared using Heck–Sonogashira coupling between *meso*-bromoporphyrin **20** and the arylacetylenes **21a** and **21b** (Scheme 3).[27] Acetylene linked porphyrin dimer **23** was synthesised *via* coupling of trimethylsilylacetylene to **20**, deprotection and a second Pd-catalysed reaction of this with another equivalent of **20** (Scheme 3). Dimer **23** was isolated in 70% yield. Therien and coworkers have previously reported the synthesis of the phenyl (rather than the 3,5-di-*tert*-butylphenyl) analogue of this dimer.[28]

Electronic absorption and emission spectra

The electronic spectra of compounds **5**–**10** are summarised in Table 1. Data for porphyrin dimers **18** and **23** are also included. A porphyrin–aryl connection which provides efficient electronic communication will lead to a large change of the porphyrin electronic spectra due to conjugation into the benzene ring. Selected absorption spectra are shown in Fig. 1. Conjugation between the porphyrin and the aryl substituent is manifested in three ways: (i) change in positions of absorption and emission maxima relative to unsubstituted porphyrin **10**; (ii) change in positions of absorption maxima on incorporation of the nitro group; (iii) change in the oscillator strength of absorptions, since the addition of conjugated connections to the *meso* positions of porphyrins generally intensifies the Q band by increasing the a_{1u}/a_{2u} orbital separation.[1c]

(i) Both the Q and B bands of all the porphyrin derivatives show a large red shift relative to the core porphyrin **10**. Azo compounds **5a**–**c** display by far the largest shifts, and in **5b** the Soret band is widely split (Fig. 1a), indicating strong conjugation with the aryl substituent and suggesting this link provides the best electronic overlap. There is little difference between the absorption spectra of compounds **6**–**9**. In general, the red shift increases in the order: alkene **8** < imine **6** ≈ imine **7** < acetylene **9** < azo **5**, a trend which may be explained by decreasing steric bulk of the porphyrin-to-benzene bridge.

(ii) The *para*-nitro group gives an additional red shift in all cases. The magnitude of this change should give an indication of the extent of communication between the porphyrin and the

Table 1 Summary of electronic spectra and torsional parameters for porphyrins **5**–**10**, **18** and **23**[a]

Compound	$-X_1X_2-$	–Y	λ_{maxB}/nm	λ_{maxQ}/nm	f_B	f_Q	λ_{em}/nm	Φ_f	θ_{AB}/°	θ_{BC}/°	θ_{AC}/°
5a	N=N	H	457	655	1.74	0.20	640	0.001	9.7 (0.3)	5.9 (0.2)	4.6 (0.5)
5b	N=N	NO_2	415, 485	692	1.71	0.31	645	0.0004	(0.4)	(0.2)	(0.6)
5c	N=N	C≡CTMS	469	672	1.52	0.22	638	0.0009	26.1 (0.3)	5.0 (0.1)	22.2 (0.4)
6a	N=CH	H	432	616	0.98	0.11	627	0.004	(22.1)	(7.4)	(29.4)
6b	N=CH	NO_2	425	642	1.39	0.12	665	0.002	(19.0)	(10.9)	(29.4)
7a	CH=N	H	438	623	1.34	0.11	640	0.015	36.3 (40.2)	24.7 (1.4)	60.7 (39.0)
7b	CH=N	NO_2	447	634	0.98	0.13	664	0.022	(40.1)	(0.8)	(39.6)
8a	CH=CH	H	435	614	1.27	0.11	628	0.101	41.6 (57.8)	14.7 (20.2)	44.7 (37.9)
8b	CH=CH	NO_2	434	628	1.36	0.09	650	0.003	(57.8)	(19.6)	(38.5)
9a	C≡C	H	439	623	1.33	0.12	627, 681	0.175	—	—	(<0.1)
9b	C≡C	NO_2	452	637	2.16	0.24	628, 682	0.017	—	—	(<0.1)
10	H	—	418	586	1.22	0.06	594, 646	0.100	—	—	—
18	N=CH	—	427, 443	663	1.18	0.15	624	0.004	(16.8)	(52.9)	(36.1)
23	C≡C	—	415, 481	710	1.62	0.25	730	0.070	—	—	(0.4)

[a] λ_{maxB}, λ_{maxQ}, f_B, f_Q, λ_{em} and Φ_f are the absorption maxima, oscillator strengths, emission maxima and fluorescence quantum yield in CH_2Cl_2–1% pyridine. λ_{maxB}, λ_{maxQ}, f_B and f_Q refer to the porphyrin B and Q bands; in cases with several Q band maxima, the longest wavelength peak is listed here. Oscillator strengths in dimers **18** and **23** are per porphyrin macrocycle. θ_{AB}, θ_{BC} and θ_{AC} are the interplane angles as defined in Fig. 2 from X-ray crystallographic analysis (and from MM2 molecular mechanics calculations).

aryl substituent. Replacement of a hydrogen by a nitro group in the azo-linked system gives the largest Q band shift of 37 nm, comparing **5a** and **5b** (Fig. 1a and Table 1), which is about twice that for compounds **6**–**9**, reinforcing our conclusion that the azo link provides exceptionally efficient conjugation. The presence of a nitro group, or a nitrogen in the link, leads to a large reduction in fluorescence quantum yield Φ_F, the only exceptions being imines **7a** and **7b**, where the nitro compound is more fluorescent. Perhaps here the addition of the nitro group favours interaction of the imine nitrogen with the benzene ring, reducing electronic communication with, and quenching of, the porphyrin.

(iii) The increase in the Q band oscillator strength f_Q relative to that of **10** indicates the effectiveness of conjugation between the porphyrin and benzene.† Again, an increase in oscillator strength on addition of the *para*-nitro group would also testify to good electronic communication across the conjugated system. There is a general increase in Soret and Q-band oscillator strengths relative to unsubstituted porphyrin **10** (Table 1). The effect is largest in *para*-nitro phenylacetylene **9b** and azo compounds **5a**–**c**. The intensification of the Q-band in the azo compounds again reveals the strong conjugation between porphyrin and benzene ring.

The absorption spectra of porphyrin dimers **18** and **23** are compared with those of their monomer analogues in Fig. 1b and 1c respectively. The acetylene linked dimer **23** shows a large red-shift, intensification of the Q band oscillator strength and a splitting of the Soret compared to *meso*-phenylethynyl porphyrin **9a** (Fig. 1c), which indicates that there is strong conjugation between the porphyrin rings. Imine dimer **18** has an absorption spectrum which is similar to the *meso*-aryl imine porphyrins **6a** and **7a** (Fig. 1b). This can be explained by the twisting of the *N*-porphyrin ring in a similar manner to that seen in *N*-benzalanilines, limiting the conjugation between the porphyrins. However, as for **6b**, the long tail to the absorption to longer wavelengths, and the increase in Q band oscillator strength, suggest that some of the dimer exists in a planar more conjugated conformation.

Crystal structures and molecular mechanics calculations

Electronic conjugation requires efficient orbital overlap, and is maximised if the π-system is planar. The planarity of the *meso*-arylporphyrins **5**–**9** and porphyrin dimers **18** and **23** was assessed by X-ray crystallography and by molecular mechanics modelling using the MM2 force field. Crystallographic data for **5a**, **5c**, **7a** and **8a** are summarised in Table 2. We were unable to grow satisfactory crystals of the remaining compounds.

The planarity was evaluated by measuring angles between the mean planes of the porphyrin core and C–X–X–C bridge, θ_{AB} and between the planes of the C–X–X–C link and the benzene ring, θ_{BC}, as illustrated in Fig. 2. In addition, the angle between the porphyrin ring and benzene ring, θ_{AC}, was also measured. Note that θ_{AC} is not always the sum or difference of $\theta_{AB} \pm \theta_{BC}$, because these are dihedral angles between least-squares planes; although the major contribution to θ_{AB} and θ_{BC} is torsion about the bond between pairs of rings, other minor tilting factors are also included. These torsional parameters are listed in Table 1, from X-ray crystallography, where available, and from molecular mechanics.

The acetylene linked systems are calculated to be essentially planar ($\theta_{AC} = 0$), but the barrier to rotation is probably small. The crystal structures of several *meso*-arylethynylporphyrins have been reported.[7,29–31] These structures have θ_{AC} values in the range 3.5–60° (mean 30.4° for all 9 observations), showing that the electronic preference for planarity is easily compromised by crystal packing interactions.

The calculated structures of all three azo compounds also show very small deviations from planarity of less than 0.5°. The X-ray structure of azo compound **5a** (Fig. 3) shows an almost planar geometry across the azo bond ($\theta_{AB} = 9.7°$; $\theta_{BC} = 5.9°$), whereas that of **5c** is more twisted ($\theta_{AB} = 26.1°$; $\theta_{BC} = 5.0°$). These values are significantly larger than those predicted by our modelling, but agree well with values of 5–15° found for *E*-azobenzene.[32] The planarity of these azoporphyrins is consistent with a high degree of conjugation.

For alkene linked porphyrin **8a**, modelling predicts $\theta_{AB} = 57.8°$ and $\theta_{BC} = 20.2°$. The X-ray structure of **8a** (Fig. 3) indicates that molecular mechanics exaggerates the distortion, as in the crystal $\theta_{AB} = 41.6°$ and $\theta_{BC} = 14.7°$. The shortest H–H contacts (Fig. 4) are H_A–H_B (2.32 Å) and H_B–$_C$ (2.15 Å); both these contacts are close to the sum of the van der Waals radii‡ so are likely to contribute towards the nonplanarity. The other H–H distances H_D–H_E (2.73 Å) and H_E–H_F (2.44 Å) are significantly longer.

Our molecular mechanics calculations gave least realistic geometries for the imines, where electronic effects due to the interaction of the imine nitrogen with the aromatic system are important, as well as steric effects. MM2 calculations predict imines **7a**,**b** to have $\theta_{AB} = 40.1°$ and $\theta_{BC} \approx 0$, which seems

† Oscillator strength, *f*, was calculated using the equation:

$$f = 4.319 \times 10^{-9}\, A/n$$

where *A* is the integrated absorption band (plotted as ε / cm^{-1}), and *n* is the solvent refractive index (1.42 for CH_2Cl_2).

‡ Using van der Waals radii of H = 1.10 Å, C = 1.77 Å, N = 1.64 Å from Ref. 44.

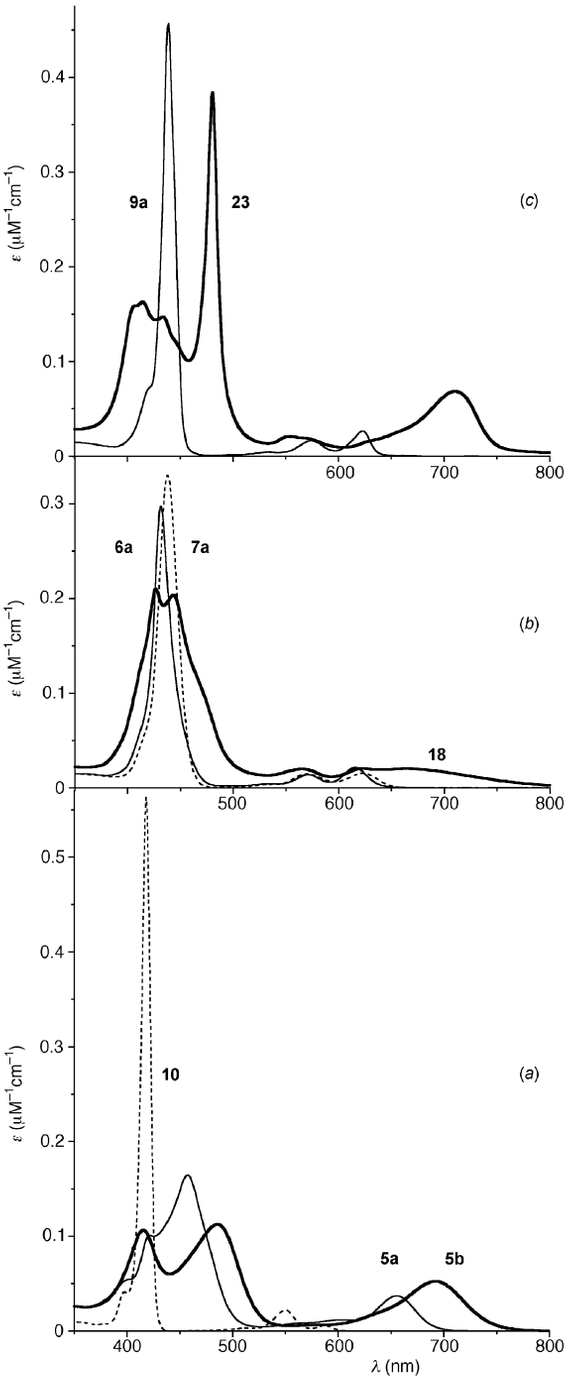

Fig. 1 Absorption spectra in CH_2Cl_2–1% pyridine of *a*) **5a** (plain), **5b** (bold) and **10** (dashed); *b*) **6a** (plain), **7a** (dashed) and **18** (bold); *c*) **9a** (plain) and **23** (bold).

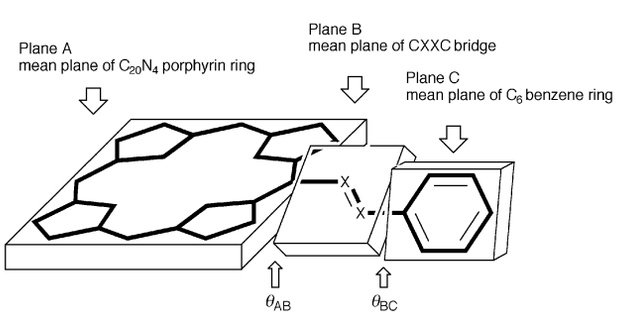

Fig. 2 Definition of torsional angles θ_{AB} and θ_{BC}.

unlikely given the large distortions of the *N*-phenyl ring in benzalanilines. The X-ray structure of **7a** (Fig. 3) shows $\theta_{AB} = 36.3°$ and $\theta_{BC} = 24.7°$. As in **8a**, the shortest H–H distances are H_A–

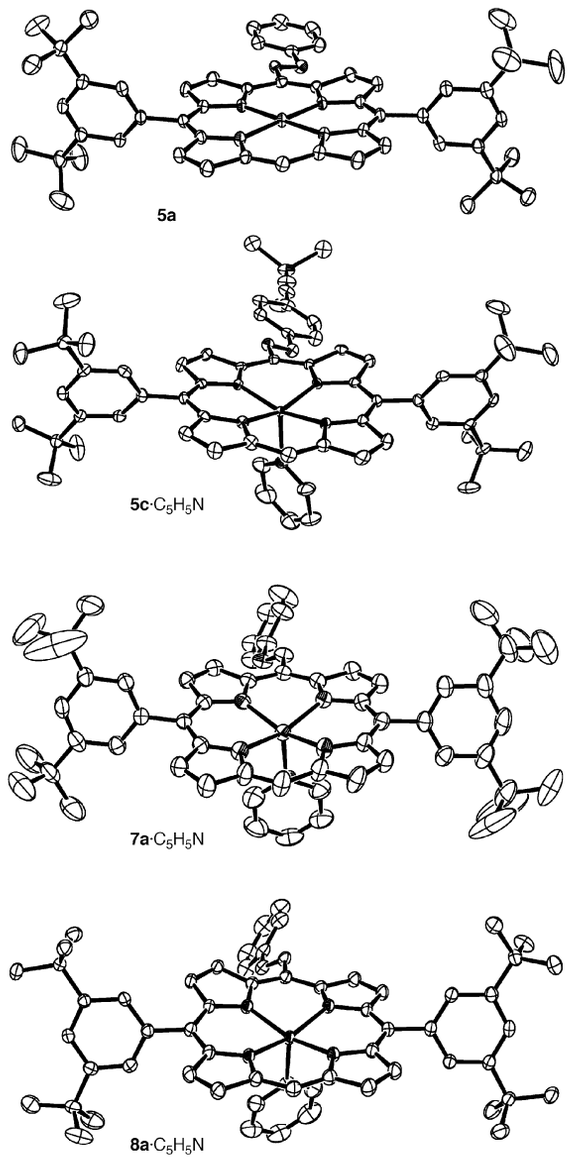

Fig. 3 X-Ray structure of **5a** and the pyridine complexes of **5c**, **7a** and **8a** (50% probability ellipsoids, H atoms and solvent molecules omitted for clarity).

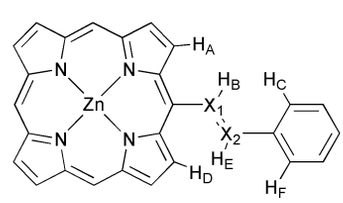

Fig. 4 Short intramolecular H–H contacts in porphyrins **6**–**9**.

H_B (2.23 Å) and H_B–H_C (2.07 Å), which are again within van der Waals contact. The H_B–H_C distance in imine **7a** is shorter than that in alkene **8a**, despite the greater θ_{BC} in the imine, due to the shorter length of the C=N bond (1.25 Å) in **7a** compared with the C=C bond (1.34 Å) in **8a**. This short C=N bond increases the steric congestion and nonplanarity. The discrepancy between predicted and observed structures casts doubt on the calculated geometry of imines **6a**, **6b** and **18**, although the nonplanarity of these systems is not necessarily the same in the solid state (as determined experimentally by crystallography) as in isolated molecules (as deduced from molecular mechanics calculations), because intermolecular interactions are ignored in the calculations and may have a significant effect in the solid state.

Table 2 Crystallographic data for compounds **5a**, **5c**, **7a** and **8a**§

	5a	**5c**	**7a**	**8a**
Formula	$C_{54}H_{56}N_6Zn{\cdot}0.75C_5H_{12}$	$C_{59}H_{64}N_6SiZn{\cdot}C_5H_5N{\cdot}C_5H_{12}$	$C_{55}H_{57}N_5Zn{\cdot}1.5C_5H_5N{\cdot}0.5C_5H_{12}$	$C_{56}H_{58}N_4Zn{\cdot}C_5H_5N{\cdot}CHCl_3$
Formula weight	908.53	1101.91	1008.15	1050.97
Crystal system	Triclinic	Triclinic	Orthorhombic	Monoclinic
Space group	$P\bar{1}$	$P\bar{1}$	$P2_12_12_1$	$P2_1/c$
a/Å	12.780(8)	13.3930(7)	15.0697(8)	15.839(3)
b/Å	14.281(7)	13.4790(5)	19.5369(10)	19.805(5)
c/Å	14.546(8)	17.9480(9)	20.9405(11)	18.687(4)
α/deg	97.162(6)	95.685(3)	90	90
β/deg	97.805(6)	95.402(2)	90	111.46(1)
γ/deg	103.870(6)	104.110(3)	90	90
V/Å^3	2519.2(2)	3103.3	6165.2(6)	5455.6(5)
Z	2	2	4	4
T/K	150	150	150	150
Reflections measured	9336	23098	39754	24767
Unique reflections	9336 (R_{int} = 0.00)	11907 (R_{merge} = 0.048)	16470 (R_{int} = 0.05)	11180 (R_{int} = 0.03)
R_1	0.0870	0.0592	0.0869	0.0579
Rw_2	0.2092	0.0659	0.2115	0.0692

The calculated structure for imine dimer **18** has twists between the imine bond atoms and the *N*-porphyrin ring, θ_{AB}, and the *C*-porphyrin ring, θ_{BC}, of 16.8° and 52.9° respectively. With an even greater value of θ_{AB} expected in the actual structure, it is not surprising that the absorption spectrum of **18** shows only weak conjugation.

Conclusions

Analysis of the electronic spectra of porphyrin–aryl compounds **5**–**9** shows that the azo-link allows most efficient π-overlap between the porphyrin and the aryl moiety. This is manifested by strong red shifts in the absorption bands relative to the other porphyrins, a large increase in oscillator strength of the Q band and a further red shift and intensification of the Q band on addition of a nitro group comparing compounds **5a** and **5b**. The X-ray crystal structure of azo compounds **5a** and **5c** show that the azo link is almost coplanar with the porphyrin macrocycle, supporting the spectral evidence for strong electronic communication.

Alkene and imine links do not provide as good conjugation as the azo bridge. The crystal structures of imine linked porphyrin **7a** and alkene linked **8a** both show a large twist across the bridging unit, explaining the reduced conjugation observed for these compounds. For **8a** this can be explained on steric grounds and the structure is predicted with reasonable accuracy by a simple molecular mechanics model. However, additional distortions are found in imine **7a**, perhaps due to interactions between the nitrogen lone pair and the adjacent benzene ring which are not adequately reproduced by the MM2 force field.

Acetylene linked porphyrin dimer **23** shows strong communication between the porphyrin rings. The nonplanarity expected in imine linked porphyrin dimer **18**, due to steric and electronic factors, is evident in its absorption spectrum, which shows very limited conjugation. The results reported here indicate that azo-linked porphyrin oligomers such as **14** should be even more conjugated than their alkyne-linked analogues, but viable routes to these azo-linked systems have yet to be discovered.

Experimental

UV measurements were carried out using a Perkin Elmer Lambda 14P spectrophotometer. Fluorescence measurements were carried out on a Fluoro-Max 2 spectrofluorimeter, and fluorescence quantum yields were measured relative to tetraphenylporphyrin in benzene (Φ_F = 0.11).[33] ^{1}H and ^{13}C NMR spectra were obtained using Bruker AM-200, 400 or 500 MHz instruments using deacidified deuterochloroform; coupling constants J are quoted in Hertz. FAB mass spectra were obtained on a VG Autospec from a 3-nitrobenzyl alcohol matrix in Oxford or by the EPSRC service at Swansea. MALDI-TOF mass spectra were recorded on a Micromass Tof Spec 2E mass spectrometer from anthracene-1,8,9-triol matrix. Only molecular ions and major peaks are reported. IR spectra were recorded in KBr discs using a Perkin Elmer Paragon 1000 spectrophotometer. None of the solids reported here melt below 350 °C. Molecular modelling calculations were run on Oxford Molecular Cache software version 4.1, and minimised using molecular mechanics employing a conjugate gradient optimisation method with the augmented MM2 force field to a convergence of 1×10^{-5} kcal mol^{-1}.

Aryldiazonium tetrafluoroborates **11a**–**c** were prepared according to the general procedure of Doyle and Bryker.[22] 5,15-Bis(3′,5′-di-*tert*-butylphenyl)porphyrin (**$H_2$10**) was prepared using the method for synthesising the bis-phenyl analogue reported by Therien and co-workers.[34] [5,15-Bis(3′,5′-di-*tert*-butylphenyl)porphyrinato]copper(II) (**Cu10**), [5,15-bis(3′,5′-di-*tert*-butylphenyl)-10-(formyl)porphyrinato]copper(II) (**Cu16**), [5,15-bis(3′,5′-di-*tert*-butylphenyl)-10-(formyl)porphyrin] (**$H_2$16**) and [5,15-bis(3′,5′-di-*tert*-butylphenyl)-10-(formyl)-porphyrinato]zinc(II) (**16**) were prepared according to the route reported by Susumu *et al.*[35] 4-Trimethylsilylethynylphenyldiazonium tetrafluoroborate **11c** was kindly provided by Dr Sally Anderson.[36]

X-Ray crystallographic data collection and processing §

Crystals of **5a** were grown by vapour diffusion of pentane into a solution of the porphyrin in $CHCl_3$. Crystals of **5c** were grown by vapour diffusion of pentanes into a solution of the porphyrin in CH_2Cl_2 containing pyridine. Crystals of **8a** were grown by vapour diffusion of methanol into a solution of the porphyrin in $CHCl_3$ containing pyridine. Data for **5a**, **5c** and **8a** were collected using an Enraf-Nonius DIP2000 Image Plate Diffractometer with graphite monochromated Mo-K_α radiation (λ = 0.7107 Å). Structure **5a** was solved using the program SIR-92[37] and refined using full-matrix least-squares on all F_0^2 data [SHELXL-93].[38] Structure **5c** was solved using SIR-92 on all 11907 reflections with $I > 5\sigma(I)$, but refined (by full matrix least squares against F [CRYSTALS][39] using only 6181 reflections with $I > 7\sigma(I)$. This gave more than 10 observations per variable and compensated for the unrealistically low estimate of σ produced by the DIP2000 diffractometer. Structure **8a** was solved using SIR-92 and refined using full-matrix least-squares on all F data [CRYSTALS]. All non-hydrogen atoms were refined anisotropically and hydrogen

§ CCDC reference numbers 173279–173282 for **5a**, **5c**, **7a** and **8a** respectively. See http://www.rsc.org/suppdata/p1/b1/b109915a/ for crystallographic files in .cif or other electronic format.

atoms were included in calculated positions with isotropic displacement parameters. Crystals of **5a** were found to contain one pentane molecule per porphyrin, disordered over two positions, with a total occupancy of 75%. **5c** crystallised with one pyridine coordinated to the porphyrin and one disordered pentane molecule. **8a** crystallised with one coordinated pyridine and one chloroform molecule in the asymmetric unit.

Crystals of **7a** were grown by vapour diffusion of pentane into a solution of the porphyrin in $CHCl_3$ containing pyridine. Data were collected using a Bruker SMART 1K CCD diffractometer using synchrotron X-rays (λ = 0.6883 Å) at Daresbury SRS Station 9.8, solved by direct methods and refined using full-matrix least-squares on all F_0^2 data [SHELXTL].[40] The crystals contained one pyridine coordinated to the zinc and one disordered pyridine at 50% occupancy, as well as a disordered pentane at 50% occupancy. The coordinated pyridine and the imine bridge are both two-fold disordered, and were successfully resolved and modelled.

[5,15-Bis(3′,5′-di-*tert*-butylphenyl)-10-phenylazoporphyrinato]-zinc(II) 5a

Zinc porphyrin **10** (75 mg, 0.10 mmol) was dissolved in THF (75 cm^3) and phenyldiazonium tetrafluoroborate **11a** (192 mg, 1.0 mmol) was added as a solution in methanol (50 cm^3). The reaction was stirred at room temperature for 15 h. The reaction mixture was then passed through a short silica plug and the solvents removed. The residue was chromatographed on silica eluting with 1 : 1 CH_2Cl_2–60–80 petroleum ether and crystallised from CH_2Cl_2 by layered addition of 1% H_2O–methanol to yield **5a** as green crystals (20 mg, 23%): $\lambda_{max}(CH_2Cl_2$–1% pyridine)/nm 457 (log ε 5.22), 602 (4.07), 655 (4.57); ν_{max}(KBr)/cm^{-1} 1594 (N=N); δ_H(500 MHz; $CDCl_3$, d_5-pyridine) 10.05 (1 H, s, *meso H*), 9.84 (2 H, d, *J* 4.7, *βH*), 9.21 (2 H, d, *J* 4.4, *βH*), 9.01 (2 H, d, *J* 4.7, *βH*), 8.93 (2 H, d, *J* 4.4, *βH*), 8.48 (2 H, d, *J* 7.7, phenyl *H*), 8.04 (4 H, d, *J* 1.8, Bu^t aryl *H*), 7.79 (2 H, t, *J* 1.8, Bu^t aryl *H*), 7.70 (2 H, t, *J* 7.7, phenyl *H*), 7.56 (1 H, t, *J* 7.7, phenyl *H*), 1.53 (36 H, s, Bu^t *H*); δ_C(125 MHz; $CDCl_3$, d_5-pyridine) 154.8, 151.3, 150.2, 149.2, 148.6, 147.4, 142.1, 133.7, 132.3, 131.8, 130.22, 130.20, 130.0, 129.4, 129.1, 124.2, 122.9, 120.8, 108.9, 35.1, 31.9; *m/z* (FAB) 854 (M^+, $C_{54}H_{56}N_6Zn$ requires 854.46).

[5,15-Bis(3′,5′-di-*tert*-butylphenyl)-10-(4-nitrophenyl)azoporphyrinato]zinc(II) 5b

Porphyrin **10** (50 mg, 0.067 mmol) was dissolved in THF (60 cm^3) and the solution cooled to 0 °C. 4-Nitrophenyldiazonium tetrafluoroborate **11b** (80 mg, 0.333 mmol) was then added as a solution in methanol (40 cm^3) and the reaction stirred for 1 h. On completion, the solvents were removed and the residue chromatographed on silica eluting with CH_2Cl_2. Crystallisation from $CHCl_3$ by layered addition of 30–40 petroleum ether yielded the pure product as green crystals (14 mg, 23%): $\lambda_{max}(CH_2Cl_2$–1% pyridine)/nm 415 (5.02), 485 (5.05), 692 (4.71); ν_{max}(KBr)/cm^{-1} 1592 (N=N), 1520 (NO_2), 1334 (NO_2); δ_H(500 MHz; $CDCl_3$, d_5-pyridine) 10.12 (1 H, s, *meso H*), 9.92 (2 H, d, *J* 4.7, *βH*), 9.26 (2 H, d, *J* 4.4, *βH*), 9.06 (2 H, d, *J* 4.7, *βH*), 8.95 (2 H, d, *J* 4.4, *βH*), 8.54 (2 H, d, *J* 8.8, phenyl *H*), 8.47 (2 H, d, *J* 8.8, phenyl *H*), 8.09 (4 H, d, *J* 1.8, Bu^t aryl *H*), 7.85 (2 H, d, *J* 1.8, Bu^t aryl *H*), 1.57 (36 H, s, Bu^t *H*); δ_C(125 MHz; $CDCl_3$, d_5-pyridine) 157.6, 152.2, 150.2, 149.2, 148.9, 147.6, 141.7, 134.5, 132.3, 132.2, 130.5, 129.9, 128.1, 126.1, 125.3, 125.2, 122.9, 121.2, 111.5, 35.2, 32.0; *m/z* (FAB) 899 (M^+, $C_{54}H_{55}N_7O_2Zn$ requires 899.45).

[5,15-Bis(3,5-di-*tert*-butylphenyl)-10-(4-trimethylsilylethynylphenyl)azoporphyrinato]zinc(II) 5c

Compound **10** (150 mg, 0.20 mmol) was dissolved in THF (150 cm^3) and 4-trimethylsilylethynylphenyldiazonium tetrafluoroborate **11c** (288 mg, 1.0 mmol) was then added as a solution in methanol (100 cm^3) and the reaction stirred at room temperature for 2 h. After this time, the mixture was passed through a short silica plug and the solvents removed. The residue was chromatographed on silica eluting with CH_2Cl_2–60–80 petroleum ether (1 : 1) and crystallised from chloroform by layered addition of 30–40 petroleum ether to yield the pure product as green crystals (52 mg, 27%). $\lambda_{max}(CH_2Cl_2)$/nm 418 (log ε 4.98), 463 (5.20), 646 (4.58); δ_H(500 MHz; $CDCl_3$, d_5-pyridine) 10.16 (1 H, s, *meso H*), 9.90 (2 H, d, *J* 4.7, *βH*), 9.33 (2 H, d, *J* 4.5, *βH*), 9.15 (2 H, d, *J* 4.7, *βH*), 9.08 (2 H, d, *J* 4.5, *βH*), 8.41 (2 H, d, *J* 8.3, *p*-NO_2 phenyl *H*), 8.15 (4 H, d, *J* 1.7, Bu^t aryl H), 7.89 (2 H, t, *J* 1.7, Bu^t aryl H), 7.86 (2 H, d, *J* 8.3, *p*-NO_2 phenyl *H*), 1.62 (36 H, s, Bu^t *H*), 0.39 (9 H, s, TMS); δ_C(125 MHz; $CDCl_3$, d_5-pyridine) 153.9, 151.5, 150.4, 149.5, 149.0, 147.1, 141.6, 134.0, 133.3, 132.9, 132.2, 130.6, 130.0, 129.6, 125.5, 124.5, 123.0, 121.3, 108.9, 105.3, 97.3, 35.3, 32.0, 0.3; *m/z* (FAB) 951 (M^+, $C_{59}H_{64}N_6SiZn$ requires 950.7).

[5,15-Bis(3′,5′-di-*tert*-butylphenyl)-10-(nitro)porphyrinato]-zinc(II)

The most successful conditions for *meso*-mononitration were similar to those reported by Cowan and Sanders.[41] Free base porphyrin $\mathbf{H_2}$10 (0.607 g, 0.88 mmol) was added to a vigorously stirred mixture of conc. HNO_3 (60 cm^3) and acetic acid (60 cm^3) at 0 °C. The mixture was stirred for 7 h, maintaining the temperature at 0–4 °C, after which time the reaction mixture was poured into iced water. The porphyrin product was extracted with CH_2Cl_2, washed with water, and the organic layer evaporated to dryness to give crude 5,15-bis(3′,5′-di-*tert*-butylphenyl)-10-(nitro)porphyrin. $\lambda_{max}(CH_2Cl_2)$/nm 416 (log ε 5.56), 514 (4.36), 552 (3.91), 585 (3.96), 642 (3.62); ν_{max}(KBr)/cm^{-1} 1525 (NO_2), 1363 (NO_2); δ_H(250 MHz; $CDCl_3$) 10.37 (1 H, s, *meso H*), 9.40 (2 H, d, *J* 4.7, *βH*), 9.37 (2 H, d, *J* 5.0, *βH*), 9.13 (2 H, d, *J* 5.0, *βH*), 9.08 (2 H, d, *J* 4.7, *βH*), 8.12 (2 H, d, *J* 1.8, aryl *H*), 7.90 (2 H, t, *J* 1.8, aryl *H*), 1.60 (36 H, s, Bu^t *H*), −2.84 (2 H, s, N*H*); *m/z* (MALDI-TOF) 732.1 (M^+, $C_{48}H_{53}N_5O_2$ requires 731.97).

All the product from the nitration was dissolved in $CHCl_3$ (100 cm^3) and $Zn(OAc)_2{\cdot}2H_2O$ (0.970 g, 4.42 mmol) in methanol (10 cm^3) was added. The solution was stirred at room temperature for 30 min. The reaction mixture was passed through a silica plug to remove excess zinc residues, then purified by column chromatography (silica, 12 : 1 : 0.5 60–80 petroleum ether–EtOAc–pyridine). The product was eluted as a dark purple solution and recrystallised from $CHCl_3$–methanol to yield [5,15-bis(3′,5′-di-*tert*-butylphenyl)-10-(nitro)porphyrinato]zinc(II) (0.551 g, 78% over two steps). $\lambda_{max}(CH_2Cl_2$–1% pyridine)/nm 318 (log ε 4.25), 427 (5.21), 561 (4.06), 611 (3.80); ν_{max}(KBr)/cm^{-1} 1513 (NO_2), 1328 (NO_2); δ_H(500 MHz; $CDCl_3$, d_5-pyridine) 10.19 (1 H, s, *meso H*), 9.33 (2 H, d, *J* 4.7, *βH*), 9.28 (2 H, d, *J* 4.4, *βH*), 9.04 (2 H, d, *J* 4.7, *βH*), 8.98 (2 H, d, *J* 4.4, *βH*), 8.00 (4 H, d, *J* 1.8, aryl *H*), 7.80 (2 H, t, *J* 1.8, aryl *H*), 1.51 (36 H, s, Bu^t *H*); δ_C(125 MHz; $CDCl_3$, d_5-pyridine) 151.8, 150.7, 149.4, 148.7, 144.7, 141.5, 134.5, 132.8, 132.5, 129.9, 129.2, 128.2, 124.2, 121.1, 109.8, 35.1, 31.8; *m/z* (FAB) 795 (M^+, $C_{48}H_{51}N_5O_2Zn$ requires 795.34).

[5,15-Bis(3′,5′-di-*tert*-butylphenyl)-10-(amino)porphyrinato]-zinc(II) 13

Reduction of the nitro group to obtain the amine was performed using the successful procedure reported by both Baldwin and co-workers,[42] and Arnold's group.[43] [5,15-Bis(3′,5′-di-*tert*-butylphenyl)-10-(nitro)porphyrinato]zinc(II) (0.480 g, 0.604 mmol) was dissolved in CH_2Cl_2 (200 cm^3) and methanol (200 cm^3) and 10% Pd on carbon (320 mg) was added. The mixture was degassed and $NaBH_4$ (0.571 g, 15.5 mmol) added in portions over 20 min. Stirring was continued for 1.5 h at room temperature. The Pd/carbon was then filtered off, the filtrate washed with water and the organic phase evaporated to

dryness. Pure **13** was obtained by recrystallisation from CH_2Cl_2–methanol (0.385 g, 83%). λ_{max}(CH_2Cl_2–1% pyridine)/nm 306 (log ε 4.17), 353 (4.08), 432 (5.28), 542 (3.98), 646 (4.09); ν_{max}(KBr)/cm^{-1} 3389 (NH_2); δ_H(500 MHz; $CDCl_3$, d_5-pyridine) 9.22 (1 H, s, *meso H*), 9.05 (2 H, d, *J* 4.2, *βH*), 8.81 (2 H, d, *J* 4.2, *βH*), 8.68 (2 H, d, *J* 4.2, *βH*), 8.55 (2 H, d, *J* 4.2, *βH*), 7.91 (4 H, d, *J* 1.7, aryl *H*), 7.71 (2 H, d, *J* 1.7, aryl *H*), 3.91 (2 H, s, N*H*$_2$), 1.50 (36 H, s, Bu^t *H*); δ_C(125 MHz; $CDCl_3$, d_5-pyridine) 153.0, 149.1, 148.5 (2C), 142.3, 139.6, 133.5, 133.4, 130.5, 129.6, 129.4, 122.6, 121.5, 120.5, 99.9, 35.1, 31.9; *m*/*z* (FAB) 765 (M^+, $C_{48}H_{53}N_5Zn$ requires 765.36).

[5,15-Bis(3′,5′-di-*tert*-butylphenyl)-10-(phenylmethylidene amino)porphyrinato]zinc(II) 6a

Toluene (15 cm^3) and benzaldehyde **15a** (0.26 cm^3, 2.56 mmol) were added to aminoporphyrin **13** (0.073 g, 0.085 mmol) and Amberlyst 15 (30 mg) under argon and the mixture heated to reflux for 3 h over a Soxhlet apparatus containing 4 Å molecular sieves. The solids were filtered off and the product chromatographed in 10 : 1 : 0.1 60–80 petroleum ether–EtOAc–pyridine. Recrystallisation from $CHCl_3$–methanol yielded the pure product, **6a** (0.049 g, 68%). λ_{max}(CH_2Cl_2–1% pyridine)/nm 432 (log ε 5.47), 571 (4.14), 616 (4.33); ν_{max}(KBr)/cm^{-1} 1591 (C=N); δ_H(500 MHz; $CDCl_3$, d_5-pyridine) 9.95 (1 H, s, *meso H*), 9.37 (2 H, d, *J* 4.5, *βH*), 9.25 (2 H, d, *J* 4.5, *βH*), 9.04 (2 H, d, *J* 4.5, *βH*), 9.01 (1 H, s, N=C*H*), 8.98 (2 H, d, *J* 4.5, *βH*), 8.41 (2 H, d, *J* 7.0, phenyl *H*), 8.10 (4 H, d, *J* 2.0, Bu^t aryl *H*), 7.81 (2 H, t, *J* 2.0, Bu^t aryl *H*), 7.43 (3 H, m, phenyl *H*), 1.65–1.55 (36 H, s, Bu^t *H*); δ_C(125 MHz; $CDCl_3$, d_5-pyridine) 168.3, 150.7, 150.3, 150.1, 148.5, 143.4, 142.5, 137.1, 134.1, 133.0, 131.9, 131.6, 131.2, 130.3, 129.6, 129.3, 128.1, 121.9, 120.6, 104.0, 35.2, 32.0; *m*/*z* (MALDI-TOF) 853.8 (M^+, $C_{55}H_{57}N_5Zn$ requires 853.47).

[5,15-Bis(3′,5′-di-*tert*-butylphenyl)-10-(4-nitrophenylmethylideneamino)porphyrinato]zinc(II) 6b

Toluene (15 cm^3) was added to **13** (0.075 g, 0.098 mmol), 4-nitrobenzaldehyde **15b** (0.442 g, 2.93 mmol) and Amberlyst 15 (approx. 30 mg) under argon and the mixture heated to reflux for 1.5 h over a Soxhlet apparatus containing 4 Å molecular sieves. The solids were filtered off and the product chromatographed in 10 : 1 : 0.1 60–80 petroleum ether–EtOAc–pyridine. Recrystallisation from CH_2Cl_2–methanol yielded the pure product, **6b** (0.043 g, 49%). λ_{max}(CH_2Cl_2–1% pyridine)/nm 425 (log ε 5.40), 572 (4.06), 618 (4.17), 642 (4.16); ν_{max}(KBr)/cm^{-1} 1592 (C=N), 1524 (NO_2), 1342 (NO_2); δ_H(500 MHz; $CDCl_3$, d_5-pyridine) 10.04 (1 H, s, *meso H*), 9.36 (2 H, d, *J* 4.3, *βH*), 9.29 (2 H, d, *J* 4.2, *βH*), 9.09 (2 H, d, *J* 4.2, *βH*), 9.06 (2 H, d, *J* 4.3, *βH*), 8.90 (1 H, s, N=C*H*), 8.40 (4 H, two s, phenyl *H*), 8.15 (4 H, s, Bu^t aryl *H*), 7.87 (2 H, s, Bu^t aryl *H*), 1.75–1.50 (36 H, s, Bu^t *H*); δ_C(125 MHz; $CDCl_3$, d_5-pyridine) 165.7, 150.3, 150.1, 149.2, 148.4, 145.1, 143.1, 142.1, 141.7, 132.9, 131.8, 131.3, 130.0, 129.5, 127.7, 124.2, 122.5, 122.1, 120.6, 104.8, 35.0, 31.8; *m*/*z* (MALDI-TOF) 898.8 (M^+, $C_{55}H_{56}N_6O_2Zn$ requires 898.47).

[5,15-Bis(3′,5′-di-*tert*-butylphenyl)-10-(phenyliminomethyl)porphyrinato]zinc(II) 7a

Toluene (12 cm^3) and aniline **17a** (0.56 cm^3, 6.36 mmol) were added to formylporphyrin **16** (0.099 g, 0.13 mmol) and Amberlyst 15 (approx. 30 mg) under argon and the mixture heated to reflux for 4 h over a Soxhlet apparatus containing 4 Å molecular sieves. The solids were then filtered off and the product recrystallised from CH_2Cl_2–methanol to obtain **7a** (0.085 g, 78%). λ_{max}(CH_2Cl_2–1% pyridine)/nm 438 (log ε 5.52), 570 (4.16), 622 (4.18); λ_{em}(CH_2Cl_2–1% pyridine)/nm 640 (λ_{ex} 437 nm); ν_{max}(KBr)/cm^{-1} 1590 (C=N); δ_H(500 MHz; $CDCl_3$, d_5-pyridine) 10.90 (1 H, br s, N=C*H*), 10.13 (1 H, s, *meso H*), 9.66 (2 H, br s, *βH*), 9.31 (2 H, d, *J* 4.5, *βH*), 9.03 (4 H, d, *J* 4.0, *βH*), 8.12 (4 H, s, Bu^t aryl *H*), 7.85 (2 H, s, Bu^t aryl *H*), 7.54 (2 H, m, phenyl *H*), 7.36 (3 H, m, phenyl *H*), 1.55 (36 H, s, Bu^t *H*); δ_C(125 MHz; $CDCl_3$, d_5-pyridine) 165.4, 153.6, 151.3, 150.4, 150.0, 149.3, 148.7, 142.2, 133.7, 132.5, 132.0, 130.1, 129.4, 129.1, 125.8, 123.1, 121.2, 120.9, 110.5, 108.4, 35.3, 32.0; *m*/*z* (MALDI-TOF) 853.4 (M^+, $C_{55}H_{57}N_5Zn$ requires 853.47).

[5,15-Bis(3′,5′-di-*tert*-butylphenyl)-10-(4-nitrophenyliminomethyl)porphyrinato]zinc(II) 7b

Toluene (12 cm^3) was added to **16** (0.099 g, 0.13 mmol), 4-nitroaniline **17b** (0.351 g, 2.54 mmol) and Amberlyst 15 (30 mg) under argon and the mixture heated to reflux for 3 h over a Soxhlet apparatus containing 4 Å molecular sieves. The solids were then filtered off and the product recrystallised from CH_2Cl_2–methanol to obtain **7b** (0.097 g, 85%). Found: C, 73.55: H, 6.55: N, 9.85. $C_{55}H_{56}N_6O_2Zn$ requires C, 73.52: H, 6.28: N, 9.35%; λ_{max}(CH_2Cl_2–1% pyridine)/nm 447 (log ε 5.16), 574 (3.85), 634 (4.16); λ_{em}(CH_2Cl_2–1% pyridine)/nm 667 (λ_{ex} 445 nm); ν_{max}(KBr)/cm^{-1} 1577 (C=N), 1521 (NO_2), 1338 (NO_2); δ_H(500 MHz; $CDCl_3$, d_5-pyridine) 11.06 (1 H, br s, N=C*H*), 10.16 (1 H, s, *meso H*), 9.97 (2 H, d, *J* 5.0, *βH*), 9.29 (2 H, d, *J* 5.0, *βH*), 9.07 (2 H, d, *J* 5.0, *βH*), 8.97 (2 H, d, *J* 5.0, *βH*), 8.45 (2 H, d, *J* 5.0, phenyl *H*), 8.06 (4 H, s, Bu^t aryl *H*), 7.82 (2 H, s, Bu^t aryl *H*), 7.71 (2 H, d, *J* 5.0, phenyl *H*), 1.56 (36 H, s, Bu^t *H*); δ_C(125 MHz; $CDCl_3$, d_5-pyridine) 167.1, 159.5, 151.7, 151.6, 149.9, 149.2, 148.8, 145.3, 142.0, 134.3, 132.5, 132.2, 130.1, 129.0, 125.6, 124.1, 121.8, 121.1, 109.9, 109.0, 35.2, 32.0; *m*/*z* (MALDI-TOF) 898.5 (M^+, $C_{55}H_{56}N_6O_2Zn$ requires 898.47).

[5,15-Bis(3′,5′-di-*tert*-butylphenyl)-10-(phenylethenyl)porphyrinato]zinc(II) 8a

Benzyl triphenylphosphonium bromide **19a** (0.454 g, 1.28 cm^3) and NaOMe (0.069 g, 1.28 mmol) were dissolved in DMF (10 cm^3) under argon. The solution was stirred for 30 min and then warmed to 50 °C. **16** (0.100 g, 0.13 mmol) was added dropwise as a solution in DMF (10 cm^3) and the reaction mixture heated at 85 °C for 45 min. Column chromatography on silica (1 : 1 60–80 petroleum ether–CH_2Cl_2) followed by recrystallisation from CH_2Cl_2–methanol yielded **8a** (0.069 g, 63%) as purple crystals. λ_{max}(CH_2Cl_2–1% pyridine)/nm 435 (log ε 5.52), 568 (4.21), 614 (4.22); ν_{max}(KBr)/cm^{-1} 1591 (C=C); δ_H(500 MHz; $CDCl_3$, d_5-pyridine) 10.07 (1 H, s, *meso H*), 9.84 (1 H, d, *J* 16, C=C*H*), 9.61 (2 H, d, *J* 4.5, *βH*), 9.29 (2 H, d, *J* 4.5, *βH*), 9.04 (2 H, d, *J* 3.5, *βH*), 9.03 (2 H, d, *J* 3.5, *βH*), 8.10 (4 H, d, *J* 2.0, Bu^t aryl *H*), 7.96 (2 H, d, *J* 7.5, phenyl *H*), 7.81 (2 H, t, *J* 2, Bu^t aryl *H*), 7.57 (2 H, t, *J* 7.5, phenyl *H*), 7.43 (1 H, t, *J* 7.5, phenyl *H*), 7.41 (1 H, d, *J* 16, C=C*H*), 1.60–1.50 (36 H, m, Bu^t *H*); δ_C(125 MHz; $CDCl_3$, d_5-pyridine) 150.4, 150.2, 149.9, 149.2, 148.5, 142.0, 138.7, 132.2, 131.4, 131.1, 130.3, 129.8, 129.2, 128.0, 127.0, 121.9, 120.7, 117.3, 105.5, 35.3, 32.0; *m*/*z* (MALDI-TOF) 852.6 (M^+, $C_{56}H_{58}N_4Zn$ requires 852.47).

[5,15-Bis(3′,5′-di-*tert*-butylphenyl)-10-(4-nitrophenylethenyl)-porphyrinato]zinc(II) 8b

4-Nitrobenzyl triphenylphosphonium bromide **19b** (0.512 g, 1.28 mmol) and NaOMe (0.069 g, 1.28 mmol) were dissolved in DMF (10 cm^3) under argon and the solution stirred for 30 min then warmed to 50 °C. **16** (0.100 g, 0.13 mmol) was added dropwise as a solution in DMF (10 cm^3) and the reaction mixture heated at 85 °C for 15 h. Column chromatography on silica (1 : 1 60–80 petroleum ether–CH_2Cl_2) followed by recrystallisation from CH_2Cl_2–methanol yielded **8b** (0.064 g, 56%). Found: C, 74.44: H, 6.86: N, 8.07. $C_{56}H_{57}N_5O_2Zn$ requires C, 74.60: H, 6.49: N, 7.91%; λ_{max}(CH_2Cl_2–1% pyridine)/nm 434 (log ε 5.18), 570 (4.10), 628 (4.24); λ_{em}(CH_2Cl_2–1% pyridine)/nm 652 (λ_{ex} 435 nm); ν_{max}(KBr)/cm^{-1} 1591 (C=C), 1517 (NO_2), 1339 (NO_2); δ_H(500 MHz; $CDCl_3$, d_5-pyridine) 10.11 (1 H, s, *meso H*), 9.95 (1 H, d, *J* 16, C=C*H*),

9.55 (2 H, d, *J* 4.5, *βH*), 9.31 (2 H, d, *J* 4.5, *βH*), 9.06 (2 H, d, *J* 4.5, *βH*), 9.05 (2 H, d, *J* 4.5, *βH*), 8.37 (2 H, d, *J* 8.0, phenyl *H*), 8.11 (4 H, d, *J* 2.0, Bu^t aryl *H*), 7.98 (2 H, t, *J* 8.0, phenyl *H*), 7.86 (2 H, t, *J* 2, Bu^t aryl *H*), 7.43 (1 H, d, *J* 16, C=C*H*), 1.65–1.55 (36 H, s, Bu^t *H*); δ_H(125 MHz; $CDCl_3$, d_5-pyridine) 150.8, 150.4, 150.0, 149.1, 148.8, 147.2, 144.7, 142.5, 139.1, 136.3, 132.8, 132.7, 131.7, 130.2, 129.2, 127.1, 124.7, 122.5, 120.9, 115.4, 106.5, 35.3, 32.0; *m*/*z* (FAB) 897.5 (M^+, $C_{56}H_{57}N_5O_2Zn$ requires 897.47).

Imine-linked porphyrin dimer 18

Aminoporphyrin **13** (18.1 mg, 23.6 μmol), formylporphyrin **16** (20.2 mg, 26.0 μmol) and Amberlyst 15 (20 mg) were mixed with toluene (15 cm^3) and pyridine (0.005 cm^3) then brought to reflux over a Soxhlet containing 3 Å molecular sieves. TFA (0.015 cm^3) was added and the mixture refluxed for 48 h. Et_3N (approx. 1 cm^3) was added, and the solids were filtered off and the filtrate evaporated to dryness. Column chromatography on silica in 10 : 1 : 0.1 60–80 petroleum ether–EtOAc–pyridine separated unreacted **16**, while changing to 1 : 1 60–80 petroleum ether–$CHCl_3$ was required to elute the dimer. Pure **18** (11.4 mg, 32%) was obtained by recrystallising from CH_2Cl_2 by the layered addition of methanol. λ_{max}(CH_2Cl_2–1% pyridine)/nm 427 (log ε 5.32), 443 (5.31), 565 (4.31), 622 (4.32), 663 (4.31); ν_{max}(KBr)/cm^{-1} 1591 (C=N); δ_H(500 MHz; $CDCl_3$, d_5-pyridine) 11.68 (1 H, s, N=C*H*), 10.55 (2 H, d, *J* 4.7, *βH*), 10.21 (1 H, s, *meso H*), 9.96 (1 H, s, *meso H*), 9.89 (2 H, d, *J* 4.5, *βH*), 9.35 (2 H, d, *J* 4.4, *βH*), 9.27 (2 H, d, *J* 4.4, *βH*), 9.18 (2 H, d, *J* 4.7, *βH*), 9.06 (2 H, d, *J* 4.4, *βH*), 9.05 (2 H, d, *J* 4.4, *βH*), 9.04 (2 H, d, *J* 4.5, *βH*), 8.16 (4 H, d, *J* 1.7, Bu^t aryl *H*), 8.14 (4 H, d, *J* 1.7, Bu^t aryl *H*), 7.82 (2 H, t, *J* 1.7, Bu^t aryl *H*), 7.79 (2 H, t, *J* 1.7, Bu^t aryl *H*), 1.57 (72 H, m, Bu^t *H*); δ_C(125 MHz; $CDCl_3$, d_5-pyridine) 151.6, 151.2, 150.5, 150.0, 149.8, 149.7, 149.0, 148.3, 148.2, 147.6, 144.0, 142.4, 142.0, 135.8, 134.0, 132.7, 132.2, 131.7, 131.4, 130.8, 129.9, 129.8, 128.7, 123.2, 123.1, 121.7, 120.6, 120.3, 110.8, 108.6, 103.4, 35.0, 34.9, 31.7 (2 C); *m*/*z* (MALDI-TOF) 1525.8 (M^+, $C_{97}H_{103}N_9Zn_2$ requires 1525.7).

[5,15-Bis(3′,5′-di-*tert*-butylphenyl)-10-bromoporphyrinato]-zinc(II) 20

Zinc porphyrin **10** (400 mg, 0.533 mmol) was dissolved in $CHCl_3$ (120 cm^3) and pyridine (0.5 cm^3). The solution was cooled to 0 °C and *N*-bromosuccinimide (123 mg, 0.693 mmol) added. The reaction was stirred for 15 min, quenched with acetone and then the solvents were removed under reduced pressure. The residue was washed with copious methanol to give a mixture of mono- and di-brominated products. This mixture was washed with $CHCl_3$ and both the filtrate and the remaining residue were then separately chromatographed on silica eluting with 10 : 1 : 0.1 60–80 petroleum ether–EtOAc–pyridine. The fractions containing the mono-brominated product **20** were evaporated to dryness and crystallised from $CHCl_3$ by layered addition of 30–40 petroleum ether to yield the pure product as a pink solid (263 mg, 59%): λ_{max}(CH_2Cl_2–1% pyridine)/nm 319 (log ε 4.29), 429 (5.68), 563 (4.24), 603 (3.87); δ_H(500 MHz; $CDCl_3$, d_5-pyridine) 10.05 (1 H, s, *meso H*), 9.71 (2 H, d, *J* 4.5, *βH*), 9.24 (2 H, d, *J* 4.5, *βH*), 8.98 (4 H, app. t, *J* 5.5, *βH*), 8.01 (4 H, d, *J* 1.8, aryl *H*), 7.77 (2 H, t, *J* 1.8, aryl *H*), 1.50 (36 H, s, Bu^t *H*); δ_C(125 MHz; $CDCl_3$, d_5-pyridine) 150.7, 150.6, 150.1, 149.1, 148.4, 142.0, 133.1, 132.9, 132.3, 131.7, 130.1, 123.7, 120.7, 106.0, 104.1, 35.0, 31.8; *m*/*z* (FAB) 829 (M^+, $C_{48}H_{51}N_4BrZn$ requires 829.23).

[5,15-Bis(3′,5′-di-*tert*-butylphenyl)-10-phenylethynylporphyrinato]zinc(II) 9a

$Pd_2(dba)_3$ (1.5 mg, 0.0014 mmol), PPh_3 (3.0 mg, 0.0116 mmol) and CuI (1.0 mg, 0.0058 mmol) were dried under vacuum and Et_3N (5 cm^3) added. The solution was degassed and then heated at 70 °C for 1.5 h. Simultaneously, bromoporphyrin **20** (40 mg, 0.0482 mmol) was dissolved in dry toluene (10 cm^3) and pyridine (0.3 cm^3) and the solution also degassed. Phenylacetylene **21a** (0.011 cm^3, 0.0964 mmol) was added to the porphyrin solution and the active catalyst solution transferred *via* cannula to this mixture. The reaction was heated to 80 °C and stirred under inert atmosphere for 2 h. On completion, the mixture was washed with water (2 × 20 cm^3) and the organic phase evaporated to dryness. The residue was chromatographed on silica eluting with 2 : 1 60–80 petroleum ether–CH_2Cl_2 and **9a** was then obtained as a green solid by crystallisation from $CHCl_3$ by layered addition of 30–40 petroleum ether (29 mg, 71%). λ_{max}(CH_2Cl_2–1% pyridine)/nm 439 (log ε 5.61), 574 (4.20), 623 (4.43); ν_{max}(KBr)/cm^{-1} 2194 (C≡C); δ_H(500 MHz; $CDCl_3$, d_5-pyridine) 10.10 (1 H, s, *meso H*), 9.85 (2 H, d, *J* 4.5, *βH*), 9.28 (2 H, d, *J* 4.5, *βH*), 9.05 (2 H, d, *J* 4.5, *βH*), 9.02 (2 H, d, *J* 4.5, *βH*), 8.09 (4 H, d, *J* 1.6, Bu^t aryl *H*), 8.05 (2 H, d, *J* 7.4, phenyl *H*), 7.83 (2 H, t, *J* 1.6, Bu^t aryl *H*), 7.56 (2 H, t, *J* 7.4, phenyl *H*), 7.47 (1 H, t, *J* 7.4, phenyl *H*), 1.58 (36 H, s, Bu^t *H*); δ_C(125 MHz; $CDCl_3$, d_5-pyridine) 152.0, 150.9, 150.1, 149.6, 148.6, 142.2, 133.0, 132.6, 131.7, 131.6, 130.5, 130.3, 128.8, 128.2, 124.9, 122.7, 120.8, 107.4, 99.1, 95.6, 94.1, 35.2, 32.0; *m*/*z* (FAB) 850 (M^+, $C_{56}H_{56}N_4Zn$ requires 850.47).

[5,15-Bis(3′,5′-di-*tert*-butylphenyl)-10-(4-nitrophenylethynyl)-porphyrinato]zinc(II) 9b

$Pd_2(dba)_3$ (4.0 mg, 4.3 μmol), PPh_3 (9.5 mg, 36 μmol) and CuI (3.4 mg, 18 μmol) were dissolved in Et_3N (11 cm^3) and the solution warmed at 70 °C for 30 min. **20** (60.0 mg, 72 μmol) and 4-nitrophenylacetylene **21b** (32.0 mg, 217 μmol) were dissolved in dry toluene (11 cm^3) and pyridine (0.25 cm^3) in a separate flask. The active catalyst solution was transferred to the reaction flask *via* cannula and the mixture heated at 80 °C. The solution was cooled after 1 h, filtered through a silica plug and then chromatographed in 10 : 1 : 0.1 60–80 petroleum ether–EtOAc–pyridine. Recrystallisation from $CHCl_3$ by layered addition of methanol yielded **9b** (59.7 mg, 92%). λ_{max}(CH_2Cl_2–1% pyridine)/nm 452 (log ε 5.48), 579 (4.30), 637 (4.81); λ_{em}(CH_2Cl_2–1% pyridine)/nm 649 (λ_{ex} 450 nm); ν_{max}(KBr)/cm^{-1} 2185 (C≡C), 1517 (NO_2), 1338 (NO_2); δ_H(500 MHz; $CDCl_3$, d_5-pyridine) 10.04 (1 H, s, *meso H*), 9.36 (2 H, d, *J* 4.3, *βH*), 9.29 (2 H, d, *J* 4.2, *βH*), 9.09 (2 H, d, *J* 4.2, *βH*), 9.06 (2 H, d, *J* 4.3, *βH*), 8.90 (1 H, s, N=C*H*), 8.40 (4 H, two s, phenyl *H*), 8.15 (4 H, s, Bu^t aryl *H*), 7.87 (2 H, s, Bu^t aryl *H*), 1.75–1.50 (36 H, m, Bu^t *H*); δ_C(125 MHz; $CDCl_3$, d_5-pyridine) 165.7, 150.3, 150.1, 149.2, 148.4, 145.1, 143.1, 142.1, 141.7, 132.9, 131.8, 131.3, 130.0, 129.5, 127.7, 124.2, 122.5, 122.1, 120.6, 104.8, 35.0, 31.8; *m*/*z* (MALDI-TOF) 895.6 (M^+, $C_{56}H_{55}N_5O_2Zn$ requires 895.46).

[5,15-Bis(3,5-di-*tert*-butylphenyl)-10-trimethylsilylethynylporphyrinato]zinc(II)

Bromoporphyrin **20** (300 mg, 0.362 mmol), $Pd_2(dba)_3$ (10 mg, 0.012 mmol), PPh_3 (23 mg, 0.087 mmol) and CuI (8 mg, 0.044 mmol) were dried under vacuum and then dissolved in dry toluene (75 cm^3), pyridine (2.25 cm^3) and Et_3N (35 cm^3). The solution was degassed and trimethylsilylacetylene (0.112 cm^3, 0.796 mmol) added and the reaction stirred under inert atmosphere at 45 °C for 15 h. On completion, the reaction mixture was washed with water (2 × 100 cm^3), the organic phase evaporated to dryness and the residue chromatographed on silica eluting with 60–80 petroleum ether–EtOAc–pyridine (10 : 1 : 0.1). Crystallisation from chloroform by layered addition of 1% water–methanol yielded pure [5,15-bis(3,5-di-*tert*-butylphenyl)-10-trimethylsilylethynylporphyrinato]zinc(II) as a green solid (254 mg, 83%). λ_{max}(CH_2Cl_2–1% pyridine)/nm 319 (log ε 4.24), 434 (5.50), 440 (5.47), 571 (4.13), 617 (4.12); ν_{max}(KBr)/cm^{-1} 2138 (C≡C); δ_H(500 MHz; $CDCl_3$, d_5-pyridine) 10.19 (1 H, s, *meso H*), 9.81 (2 H, d, *J* 4.5, *βH*), 9.34 (2 H, d, *J* 4.5, *βH*), 9.08 (4 H, d, *J* 4.5, *βH*), 8.11 (4 H, d, *J* 1.8, Bu^t aryl

H), 7.85 (2 H, t, *J* 1.8, Bu^t aryl *H*), 1.59 (36 H, s, Bu^t *H*), 0.64 (9 H, TMS); δ_C(125 MHz; $CDCl_3$, d_5-pyridine) 152.4, 151.0, 150.4, 149.6, 148.9, 141.8, 133.3, 132.8, 131.9, 131.0, 130.1, 122.9, 121.1, 108.6, 107.7, 100.8, 99.6, 35.3, 32.0, 0.7; *m*/*z* (FAB) 847 (M^+, $C_{53}H_{60}N_4SiZn$ requires 846.6).

[5,15-Bis(3,5-di-*tert*-butylphenyl)-10-ethynylporphyrinato]-zinc(II) 22

[5,15-Bis(3,5-di-*tert*-butylphenyl)-10-trimethylsilylethynylporphyrinato]zinc(II) (200 mg, 0.236 mmol) was dissolved in dry CH_2Cl_2 (80 cm^3) and TBAF (0.354 cm^3 of a 1 M solution in THF, 0.354 mmol) added. The reaction was stirred at room temperature for 15 min and then quenched by adding acetic acid (0.020 cm^3, 0.354 mmol). The pure product **22** was precipitated from the reaction mixture with 1% water in methanol as purple crystals (166 mg, 91%). λ_{max}(CH_2Cl_2–1% pyridine)/nm 426 (log ε 5.60), 560 (4.24); ν_{max}(KBr)/cm^{-1} 2089 (C≡C); δ_H(500 MHz; $CDCl_3$, d_5-pyridine) 10.15 (1 H, s, *meso H*), 9.78 (2 H, d, *J* 4.5, *βH*), 9.31 (2 H, d, *J* 4.5, *βH*), 9.06 (2 H, d, *J* 4.5, *βH*), 9.03 (2 H, d, *J* 4.5, *βH*), 8.08 (4 H, d, *J* 1.8, Bu^t aryl *H*), 7.82 (2 H, t, *J* 1.8, Bu^t aryl *H*), 4.15 (1 H, s, C≡C–*H*), 1.59 (36 H, s, Bu^t *H*); δ_C(125 MHz; $CDCl_3$, d_5-pyridine) 152.6, 151.2, 150.5, 149.7, 148.8, 142.4, 133.4, 132.7, 131.9, 130.8, 130.4, 122.8, 121.0, 107.8, 97.5, 87.8, 82.8, 35.4, 32.2; *m*/*z* (FAB) 774 (M^+, $C_{50}H_{52}N_4Zn$ requires 774.4).

Acetylene-linked porphyrin dimer 23

Ethynylporphyrin **22** (100 mg, 0.129 mmol), bromoporphyrin **20** (210 mg, 0.258 mmol), $Pd_2(dba)_3$ (3.4 mg, 0.004 mmol), PPh_3 (7.9 mg, 0.030 mmol) and CuI (2.9 mg, 0.015 mmol) were dried under vacuum and dissolved in dry toluene (25 cm^3), pyridine (0.5 cm^3) and Et_3N (25 cm^3). The solution was degassed and the reaction stirred under inert atmosphere for 1.5 h at 80 °C. On completion, the mixture was passed through a short silica plug and the product then separated from excess bromoporphyrin **20** on a silica column eluting with 60–80 petroleum ether–CH_2Cl_2–pyridine (10 : 1 : 0.1 and then increasing the polarity to 2 : 1 : 0.1). 1% Pyridine in chloroform was required to remove all the product from the column. Crystallisation from chloroform by layered addition of methanol yielded the pure dimer as a black solid (138 mg, 70%). λ_{max}(CH_2Cl_2–1% pyridine)/nm 415 (log ε 5.21), 434 (5.17), 481 (5.59), 710 (4.84); ν_{max}(KBr)/cm^{-1} 2155 (C≡C); δ_H(500 MHz; $CDCl_3$, d_5-pyridine) 10.48 (4 H, d, *J* 4.4, *βH*), 10.03 (2 H, s, *meso H*), 9.22 (4 H, d, *J* 4.4, *βH*), 9.14 (4 H, d, *J* 4.4, *βH*), 8.97 (4 H, d, *J* 4.4, *βH*), 8.09 (8 H, d, *J* 1.5, Bu^t aryl *H*), 7.79 (4 H, t, *J* 1.5, Bu^t aryl *H*), 1.52 (72 H, s, Bu^t *H*); δ_C(125 MHz; $CDCl_3$, d_5-pyridine) 152.6, 150.8, 150.1, 149.7, 148.6, 142.2, 133.0, 132.5, 131.4, 130.5, 129.9, 122.8, 120.7, 107.0, 101.3, 100.9, 35.1, 31.8; *m*/*z* (FAB) 1523 (M^+, $C_{98}H_{102}N_8Zn_2$ requires 1522.7).

Acknowledgements

This work was supported by the Engineering and Physical Sciences Research Council (EPSRC) and the Defence Science and Technology Laboratory (DSTL, Malvern). Dr David J. Watkin provided valuable advice on crystallography. We are also grateful to the EPSRC Mass Spectrometry Service in Swansea for FAB mass spectra.

References

1 (*a*) A. Tsuda and A. Osuka, *Science*, 2001, **293**, 79; (*b*) D. P. Arnold, *Synlett*, 2000, 296; (*c*) H. L. Anderson, *Chem. Commun.*, 1999, 2323; (*d*) M. G. Vicente, L. Jaquinod and K. M. Smith, *Chem. Commun.*, 1999, 1771; (*e*) Z. Boa and L. Yu, *Trends Polym. Sci.*, 1995, 159.
2 S. M. LeCours, H.-W. Guan, S. G. DiMagno, C. H. Wang and M. J. Therien, *J. Am. Chem. Soc.*, 1996, **118**, 1497.
3 K. S. Suslick, C.-T. Chen, G. R. Meredith and L.-T. Cheng, *J. Am. Chem. Soc.*, 1992, **114**, 6928.
4 H. L. Anderson, S. J. Martin and D. D. C. Bradley, *Angew. Chem., Int. Ed. Engl.*, 1994, **33**, 655.
5 J. R. G. Thorne, S. M. Kuebler, R. G. Denning, I. M. Blake, P. N. Taylor and H. L. Anderson, *Chem. Phys.*, 1999, **248**, 181; S. M. Kuebler, R. G. Denning and H. L. Anderson, *J. Am. Chem. Soc.*, 2000, **122**, 339.
6 H. L. Anderson, *Tetrahedron Lett.*, 1992, **33**, 1101.
7 H. L. Anderson, A. P. Wylie and K. Prout, *J. Chem. Soc., Perkin Trans. 1*, 1998, 1607.
8 L. R. Milgrom, G. Yahioglu, D. W. Bruce, S. Morrone, F. Z. Henari and W. J. Blau, *Adv. Mater.*, 1997, **9**, 313.
9 F. Z. Henari, W. J. Blau, L. R. Milgrom, G. Yahioglu, D. Phillips and J. A. Lacey, *Chem. Phys. Lett.*, 1997, **267**, 229.
10 A. Krivokapic, H. L. Anderson, G. Bourhill, R. Ives, S. Clark and K. J. McEwan, *Adv. Mater.*, 2001, **13**, 652.
11 K. Müllen and G. Wegner, *Electronic Materials: The Oligomer Approach*; Wiley-VCH, Chichester, 1998.
12 R. E. Martin and F. Diederich, *Angew. Chem., Int. Ed.*, 1999, **38**, 1350.
13 J. O. Morley, *Int. J. Quantum Chem.*, 1993, **46**, 19.
14 L.-T. Cheng, W. Tam, S. R. Marder, A. E. Stiegman, G. Rikken and C. W. Spangler, *J. Phys. Chem.*, 1991, **95**, 10643.
15 M. J. S. Dewar, *J. Am. Chem. Soc.*, 1952, **74**, 3345.
16 I. D. L. Albert, T. J. Marks and M. A. Ratner, *Chem. Mater.*, 1998, **10**, 753.
17 H. B. Bürgi and J. D. Dunitz, *Helv. Chim. Acta*, 1970, **53**, 1747.
18 M. Traetteberg, I. Hilmo, R. J. Abraham and S. Ljunggren, *J. Mol. Struct.*, 1978, **48**, 395.
19 R. Akaba, K. Tokumaru and T. Kobayashi, *Bull. Chem. Soc. Jpn.*, 1980, **53**, 1993.
20 J. O. Morley, *J. Chem. Soc., Perkin Trans. 2*, 1995, 731.
21 A. W. Johnson and D. Oldfield, *J. Chem. Soc. (C)*, 1966, 794.
22 M. P. Doyle and W. J. Bryker, *J. Org. Chem.*, 1979, **44**, 1572.
23 J.-H. Fuhrhop in *The Porphyrins*, ed. D. Dolphin, Academic Press, New York, 1978, vol. 2, ch. 5.
24 M. J. Billig and E. W. Baker, *Chem. Ind.*, 1969, 654.
25 S. Nishitani, N. Kurata, Y. Sakata, S. Misumi, M. Migita, T. Okada and N. Mataga, *Tetrahedron Lett.*, 1981, **22**, 2099.
26 L. Czuchajowski and M. Lozynski, *J. Heterocycl. Chem.*, 1988, 349.
27 R. W. Boyle, C. K. Johnson and D. Dolphin, *J. Chem. Soc., Chem. Commun.*, 1995, 527.
28 V. S.-Y. Lin, S. G. DiMagno and M. J. Therien, *Science*, 1994, **264**, 1105.
29 P. N. Taylor, A. P. Wylie, J. Huuskonen and H. L. Anderson, *Angew. Chem., Int. Ed.*, 1998, **37**, 986.
30 M. Yeung, A. C. H. Ng, M. G. B. Drew, E. Vorpagel, E. M. Breitung, R. J. McMahon and D. K. P. Ng, *J. Org. Chem.*, 1998, **63**, 7143.
31 S. M. LeCours, S. G. DiMagno and M. J. Therien, *J. Am. Chem. Soc.*, 1996, **118**, 11854.
32 C. J. Brown, *Acta Crystallogr.*, 1966, **21**, 146.
33 P. G. Seybold and M. Gouterman, *J. Mol. Spectrosc.*, 1969, **31**, 1.
34 S. G. DiMagno, V. S.-Y. Lin and M. J. Therien, *J. Org. Chem.*, 1993, **58**, 5983.
35 K. Susumu, T. Shimidzu, K. Tanaka and H. Segawa, *Tetrahedron Lett.*, 1996, **37**, 8399.
36 S. Anderson, *Chem. Eur. J.*, 2001, **7**, 4706.
37 SIR92 – A program for crystal structure solution A. Altomare, G. Cascarano, C. Giacovazzo and A. Guagliardi, *J. Appl. Crystallogr.*, 1993, **26**, 343.
38 SHELXL93 – Program for Crystal Structure Refinement. G. M. Sheldrick, Institüt für Anorganische Chemie der Universität, Tammanstrasse 4, D-3400 Göttingen, Germany, 1993.
39 CRYSTALS. D. J. Watkin, C. K. Prout, J. R. Carruthers and P. W. Better, Chemical Crystallography Laboratory, Oxford, UK, 1996.
40 G. M. Sheldrick, SHELXTL version 5, Bruker AXS Inc., Madison, Wisconsin, USA, 1997.
41 J. A. Cowan and J. K. M. Sanders, *J. Chem. Soc., Perkin Trans. 1*, 1987, 2395.
42 J. E. Baldwin, M. J. Crossley and J. DeBernardis, *Tetrahedron*, 1982, **38**, 685.
43 D. P. Arnold, R. C. Bott, H. Eldridge, F. M. Elms, G. Smith and M. Zojaji, *Aust. J. Chem.*, 1997, **50**, 495.
44 R. S. Rowland and R. Taylor, *J. Phys. Chem.*, 1996, **100**, 7384.